Proceedings World Geothermal Congress 2020+1
Reykjavik, Iceland, April - October 2021

Modeling Ground Surface Deformation at the Swiss HEATSTORE Underground Thermal Energy Storage Sites

Daniel T. Birdsell and Martin O. Saar

Geothermal Energy and Geofluids Group, Institute of Geophysics, ETH Zürich, Sonneggstrasse 5, 8092 Zürich, Switzerland

danielbi@ethz.ch

Keywords: Heat Storage, Ground Surface Deformation, Poroelasticity, Aquifer Thermal Energy Storage

ABSTRACT

High temperature (>25 °C) aquifer thermal energy storage (HT-ATES) is a promising technology to store waste heat and reduce greenhouse gas emissions by injecting hot water into the subsurface during the summer months and extracting it for district heating in the winter months. Nevertheless, ensuring the long-term technical success of an HT-ATES project is difficult because it involves complex coupling of fluid flow, heat transfer, and geomechanics. For example, ground surface deformation due to thermo- and poro-elastic deformation could cause damage to nearby infrastructure, and it has not been considered very extensively in the literature. The Swiss HEATSTORE consortium is a group of academic and industrial partners that is developing HT-ATES pilot projects in Geneva and Bern, Switzerland. Possible target formations at the Geneva site include: (a) fractured Cretaceous limestone aquifers interbedded within lower-permeability sedimentary rock and (b) Jurassic reef complex(es), also potentially fractured. In this work we offer numerical modeling support for the Geneva site. A site-specific, hydro-mechanical (HM) model is created, which uses input from the energy systems scenarios and 3D static geological modeling performed by other Swiss consortium partners. Results show that a large uplift (> 5 cm) is possible after one loading cycle, but a sensitivity analysis shows that uplift is decreased to ≤ 0.3 cm if the aquifer permeability is increased or an auxiliary well is included to balance inflow and outflow. Future work includes running coupled thermo-hydro-mechanical (THM) models for several loading and unloading cycles. The THM framework can help inform future decisions about the Swiss HT-ATES sites (e.g. the final site selection within the Geneva basin, well spacing, and operating temperature). It can also be applied to understand surface deformation in the context of geothermal energy, carbon sequestration, and at other ATES sites worldwide.

1. INTRODUCTION

There is a large carbon footprint associated with the heating and cooling sector, and aquifer thermal energy storage (ATES) represents a way to reduce CO_2 emissions while heating and cooling economically. Globally, the heating and cooling sector accounts for roughly half of the total final energy consumption, while relying primarily on fossil fuels (Fleuchaus et al., 2018). ATES shifts the seasonal timing of supply and demand in a heating system, which is useful because heat can be generated and stored when it has a low monetary or carbon cost and used later when it is more valuable. For example, summertime waste heat can be captured and stored from a power plant or industrial process that runs year-round. Later, this heat can be used for domestic and commercial wintertime heating that would otherwise use fossil fuels. ATES systems are an economical way to store thermal energy; they typically have a 2-10 year payback period, and ≥25-year lifetime (Hartog et al., 2013; Bloemendal et al., 2014). There are thousands of ATES systems in the world, and the majority operate at a relatively low temperature (<25 °C) in thick, unconsolidated aquifers in the Netherlands (Fleuchaus et al., 2018).

The GEOTHERMICA HEATSTORE project focuses on accelerating the uptake of geothermal energy and underground thermal energy storage (UTES), including ATES across 24 partners and 9 countries (Guglielmetti et al., 2020). The Swiss consortium involves two planned pilot projects for HT-ATES. The projects are located in Geneva and Bern and hope to store heat in fractured limestone and thin sandstone layers, respectively. These Swiss projects differ from the majority of previous ATES projects because of the different reservoir properties, higher operating temperatures, and deeper reservoir locations (Snijders and Drijver, 2016; Fleuchaus et al., 2018).

The aforementioned differences and complex, coupled THM processes mean that ensuring the technical success of the HT-ATES sites in Switzerland is difficult. For example, ground surface deformation can occur due to thermo- and poro-elastic expansion. The injection pressure and temperature at the Swiss HT-ATES sites are likely to be higher than at most previous ATES sites, which could lead to larger deformation than at previous sites. Although we are not aware of any field-scale observations of ground deformation at an HT-ATES site, some insight can be gained from geothermal energy sites, which also induce changes in fluid temperature and pressure during their operations. Some geothermal projects have large rates of subsidence (on the order of decimeters per year) and cause damage to nearby infrastructure (e.g. Fialko and Simons, 2000; Sarychikhina and Glowacka, 2015).

In this paper we investigate the potential for ground surface deformation at the HT-ATES pilot project in Geneva, Switzerland. In Section 2, we discuss the conceptual model of the Geneva site, which incorporates information from the heat supply and demand and the geological model. In Section 3, we present the governing equations, boundary conditions, and material properties of our HM numerical model. We acknowledge that this approach ignores the thermal expansion and plan to expand our model to include thermal coupling in future work. In Section 4, we present results for a base case and a sensitivity analysis on the injection depth, the rock's Young's modulus, the aquifer permeability, and the well operations. Section 5 provides discussion and conclusions.

2. CONCEPTUAL MODEL

Our conceptual model uses information from: (a) the thermal energy systems scenarios for the city of Geneva and (b) the static geological modeling, which is discussed in more detail in the following paragraphs. There is uncertainty in both the energy systems

scenarios and the geological models, but we incorporate information to make a somewhat-simplified, site-specific model. In this paper, we consider only the loading stage (i.e. injection of water during periods of excess heat) of the HT-ATES system. As the GEOTHERMICA HEATSTORE project progresses, more site-specific information will be incorporated into the conceptual and numerical model.

Waste heat is supplied by a waste-to-energy plant operated by the local utility in Geneva (Guglielmetti et al., 2020). When planning an ATES system that will be part of a city-wide heating strategy, it is prudent to design it to operate for decades. The supply and demand of waste heat is uncertain over the next 15-20 years in Geneva because of expansions and operational changes in the district heating network, plans to reduce fossil fuel use, and demographic changes. Currently, approximately 50 GWh/yr of heat is vented to the atmosphere and lost as waste heat. Additionally, the timing of when waste heat can be stored is a complicated function of hourly to monthly weather, operational decisions at the waste-to-energy plant, etc. Based on input from the energy system modeling scenarios (see Guglielmetti et al., 2020), we consider a loading duration of 216 days at 50 L/s injection rate, which would store approximately 50 GWh of heat if water is heated 50 °C. These fluid injection parameters are based on the waste heat at the surface and do not consider the feasibility of injecting at these rates in the subsurface.

Subsurface exploration and characterization, which has included the drilling and interpretation of the GEo-01 well to 744 m depth, informs our conceptual model (Guglielmetti et al., 2020). GEo-01 is an artesian well that flows at 50 L/s and sits within a "flower structure" of faults (Guglielmetti et al., 2020). The drilling campaign will continue in the Geneva basin, and the final location of the heat storage well(s) will likely be in an area without artesian flow and/or with fewer nearby faults. Five potential heat-storage intervals were identified by University of Geneva based on lithology, porosity, and permeability (Guglielmetti et al., 2020). In our model, we focus on the three fractured, Cretaceous limestone aquifers and the Jurassic reef complex for storage and neglect the potential storage unit in the Molasse. We combine the three Cretaceous aquifers into one of an equivalent thickness at the average depth of the three. The material properties in our model (e.g. porosity, permeability, Young's modulus, Biot coefficient) were provided by a combination of lab and field experiments or based on literature values. There are many fractures and faults in the Geneva basin and near GEo-01, which may imply a heterogeneous, anisotropic permeability field, but for simplicity we assume homogeneous, isotropic permeability for each unit in our conceptual model. We also assume a hydrostatic pressure profile. Injection occurs into either the Jurassic reef structure or the Cretaceous aquifer. The conceptual model is shown in 2D in Figure 1a.

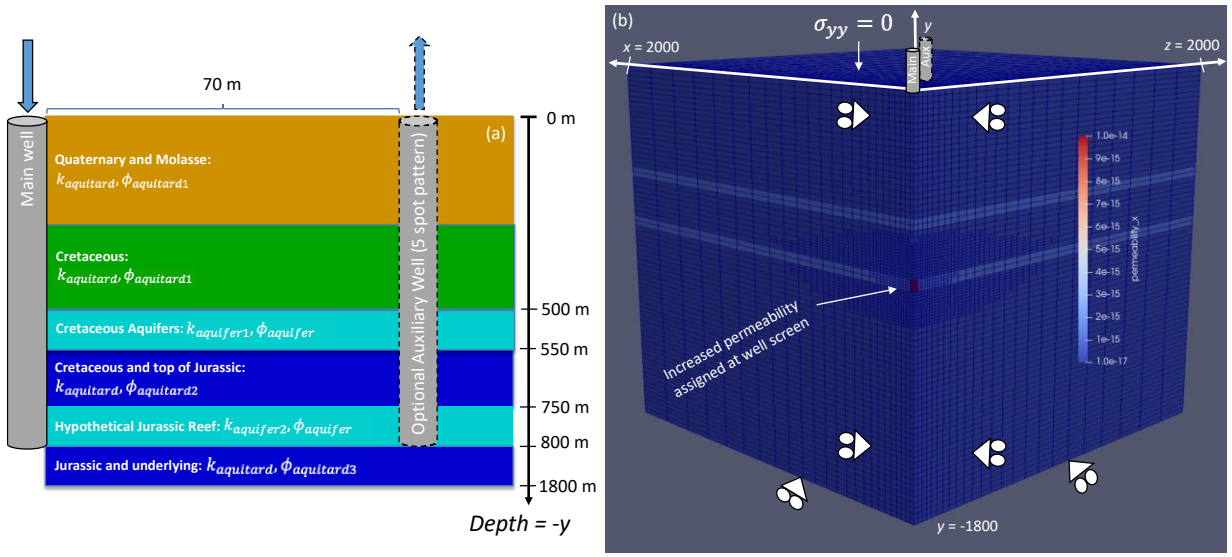

Figure 1: Depiction of the conceptual and numerical model. (a) A 2D depiction of the conceptual model, which is based on the preliminary interpretation of the GEo-01 well (Guglielmetti et al., 2020) and shows the Quaternary and Molasse (brown), Cretaceous aquitards (green), Jurassic aquitards (blue), and potential heat storage units (teal). (b) The numerical model showing the permeability and the mechanical boundary conditions (indicated with roller symbols and σ_{yy}) for the base case simulation. The numerical model has elevated permeability at the injection location and utilizes adaptive mesh refinement near large pore pressure gradients. Both subfigures show the location of the main well and an optional auxiliary well used in a sensitivity analysis.

3. NUMERICAL MODEL

HM numerical modeling is used to investigate surface uplift. We use a poroelastic formulation (Biot, 1941; Wang, 2000; Verruijt, 2013). Fluid flow is governed by the continuity equation for fluid mass and uses Darcy's equation for fluid flux:

$$\frac{\partial(\rho\phi)}{\partial t} + \rho\phi\nabla\cdot\boldsymbol{v_s} - \nabla(\rho\boldsymbol{q}) - Q = 0 \quad (1)$$

$$\boldsymbol{q} = -\frac{k}{\mu}(\nabla P - \rho\boldsymbol{g}) \quad (2)$$

where ρ is the fluid density, ϕ is the porosity, t is time, $\boldsymbol{v_s}$ is the solid skeleton velocity, $\boldsymbol{q}$ is the Darcy velocity or specific discharge, Q represents fluid sources, k is the permeability, μ is the fluid dynamic viscosity, P is the fluid pressure, and g is gravitational acceleration. Equations 1 and 2 assume that there is a single phase and a single component. The equation of state defines density as a function of pressure, for a mildly compressible fluid (i.e. liquid water).

The geomechanics are governed by the equilibrium equations with quasi-static equilibrium assumed:

$$\frac{\partial \sigma_{ji}}{\partial x_j} = -F_i \quad (3)$$

In Equation 3 index notation is used, σ_{ij} represents the components of the Cauchy stress tensor, which are positive in tension, and F_i represents the body force vector. The constitutive equation for stress accounts for the pore pressure according to Biot poroelasticity (Biot, 1941; Wang, 2000; Verruijt, 2013):

$$\sigma_{ij} = \lambda \epsilon_{kk} + 2\mu \epsilon_{ij} - \alpha P \delta_{ij} \quad (4)$$

The repeated subscript "kk" indicates a summation, ϵ_{ij} are components of the strain tensor, λ and μ are the Lamé parameters (which can be related to Young's modulus and Poisson's ratio), α is the Biot coefficient, and δ_{ij} is the Kronecker delta, which equals 0 if $i \neq j$ and 1 if $i = j$. By rearranging Equation 4, the effective stress can be defined as $\sigma'_{ij} = \lambda \epsilon_{kk} + 2\mu \epsilon_{ij} = \sigma_{ij} + \alpha P \delta_{ij}$. As is standard in poroelasticity, we assume that strains are small and reversible and are expressed as:

$$\epsilon_{ij} = \frac{1}{2}\left(\frac{\partial u_i}{\partial x_j} + \frac{\partial u_j}{\partial x_i}\right) \quad (5)$$

where u_i expresses the magnitude of deformation and x_i expresses the direction for the spatial derivative, both in the ith spatial direction.

There is a monolithic, two-way coupling between the flow and mechanics. The solid velocity (which can also be expressed as $\partial u_i / \partial t$) appears in Equation 1. The porosity in Equation 1 is a function of the mechanical strain: $\phi = 1 + (\phi_o - 1)e^{-\epsilon_{kk}}$ where ϕ_o is the initial porosity (Alger et al., 2019). The pore pressure affects the mechanics by altering the effective stress, which in turn affects the strains.

Equations 1-5 are solved using the Multiphysics Object Oriented Simulation Environment (MOOSE) (Gaston et al., 2015; Alger et al., 2019). It is a flexible, parallelized finite element solver that allows users to create their own applications. There are several examples wherein MOOSE is used to solve hydro-mechanical, thermo-mechanical, and thermo-hydro-mechanical equations that are relevant to drilling and reservoir engineering (Poulet and Veveakis, 2016; Cacace and Jacquey, 2017; Vogler et al., 2017). We use the built-in *PorousFlow* and *TensorMechanics* modules to solve the poroelastic equations in terms of pressure and displacement. We use MOOSE's adaptive mesh refinement to add discretization, where gradients of pore pressure are large, which can be seen in Figure 1b.

The numerical model domain is 2.0 km x 1.8 km x 2.0 km and represents an abstraction of the geological model, but is nevertheless based on the Geneva site. One quarter of the reservoir system is simulated to speed up simulations and simplify boundary conditions. The geological layers are assumed to be horizontal and are lumped together if they have similar hydrologic and mechanical parameters (e.g. the Quaternary and Molasse are lumped together). The three Cretaceous aquifers are lumped together and are located at a depth of 500-550 m, with a thickness equal to the total thickness of the three aquifers. The exact depth of the Jurassic reef aquifer is somewhat uncertain, but we assign it to a depth of 750-800 m in the numerical model. The permeability at the well screen elements is assigned to be one order of magnitude larger than the aquifer, which helps numerical convergence. This is a reasonable assumption if completion includes acidizing or stimulation, and the assumption likely has a small effect on the results because the elements are small. The parameters used in the base case of the numerical model are shown in Table 1 and illustrated in Figure 1a.

The boundary and initial conditions must be specified carefully because of the coupling between the hydrologic and mechanical equations. We adopt an approach wherein the initial pressure and displacement are set to zero and the perturbations in pressure and displacement are of interest. Under this approach, $P = 0$ is equivalent to hydrostatic pressure. This approach requires that gravity is set to zero. Injection is modeled as a line source along the edge of the domain (at $x = z = 0$ m, $-800 \leq y \leq -750$ m), which injects the equivalent of 50 L/s for 216 days (the actual source strength is 12.5 L/s because only one fourth of the aquifer is simulated). The injection region is visible in Figure 1b because of its larger assumed permeability. No-flux boundary conditions are applied on the planes $x = 0$ and $z = 0$ (due to symmetry) and on the top and bottom of the domain. The remaining two boundaries prescribe $P = 0$ (i.e. hydrostatic).

Table 1 – Base case model parameters

Parameter	Value	Unit
Injection Duration	216	d
Injection Rate	50	L/s
Fluid Bulk Modulus	2	GPa
Fluid Viscosity	0.001	Pa-s
Fluid Density at $P = 0$	1000	kg/s
Gravity	0	m^2/s
Aquifer Permeability ($k_{aquifer1}, k_{aquifer2}$)	10^{-15}	m^2
Aquifer Porosity ($\phi_{aquifer}$)	0.15	-
Aquitard Permeability ($k_{aquitard}$)	10^{-17}	m^2
Upper Aquitard Porosity ($\phi_{aquitard1}$)	0.02	-
Middle Aquitard Porosity ($\phi_{aquitard2}$)	0.02	-
Lower Aquitard Porosity ($\phi_{aquitard3}$)	0.01	-
Rock Young's Modulus (E)	50	GPa
Poisson's Ratio (ν)	0.3	-
Biot Coefficient (α)	1.0	-

The mechanical boundary conditions are depicted in Figure 1b: the top of the domain has no vertical load applied, the bottom of the domain has no vertical displacement, the vertical planes nearest to the well allow for vertical displacement but no displacement normal to the plane (which is a result of symmetry), and the vertical planes farthest from the well are stress-free.

4. RESULTS

The base case scenario simulates injection into the Jurassic aquifer with one, centrally-located well and assigns hydrologic and mechanical parameters based on expected or measured values in the Geneva Basin (Guglielmetti et al., 2020). The pore pressure and displacements are shown in Figure 2. Pore pressure reaches a very large value of >100 MPa near the well, and we confirm that this is reasonable for the chosen set of parameters using the Theis (1935) analytical solution. Moving horizontally away from the well in the aquifer, the pressure decreases at a decreasing rate. This large pore pressure causes poroelastic expansion and induces displacements, which are primarily vertical near the well (i.e. for a radius < 25 m, as seen in Figure 2b). At larger horizontal distances from the well, the displacements have a considerable radial component, as shown in Figures 2c and 2d. The results show that the domain is large enough that boundary effects are minimal.

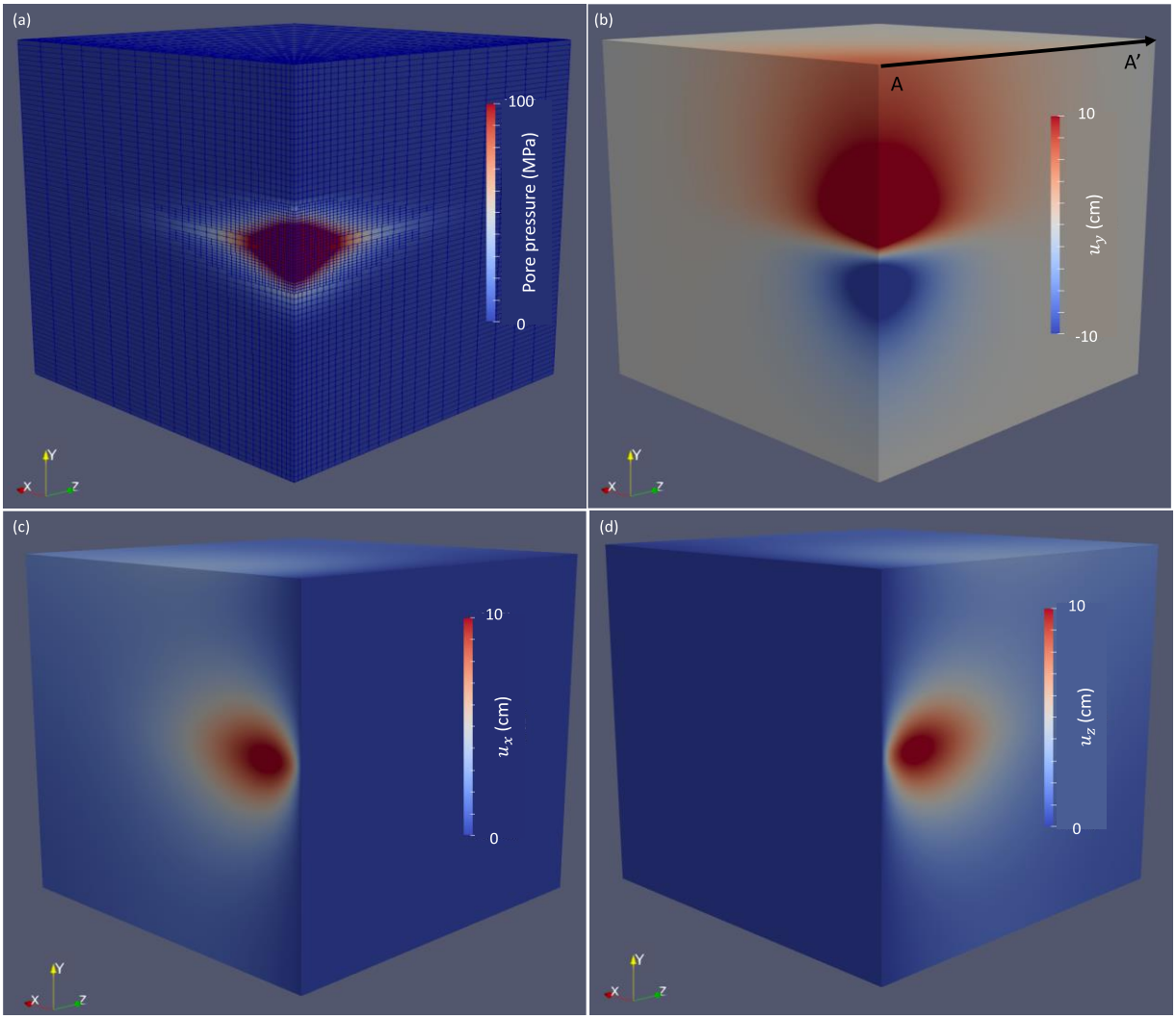

Figure 2: Base-case results for (a) pore pressure, (b) vertical displacement, (c) horizontal displacement in the *x* direction, and (d) horizontal displacement in the *z* direction at the end of a 216-day injection period. The pore pressure plot also includes the mesh, which is more discretized near the well due to adaptive mesh refinement.

We conduct a sensitivity analysis to explore the importance of aquifer depth, Young's modulus, aquifer permeability, and the well pattern that we use. The aquifer depth is perturbed from its base-case depth of 750 m (representing a hypothetical Jurassic reef complex) to a shallower depth of 500 m (representing the average depth of the three Jurassic aquifers at GEo-01). The Young's modulus is perturbed from 50 GPa to 10 GPa. The aquifer permeability is perturbed from its expected value of 10^{-15} m^2 to 10^{-13} m^2, because the limestone units at Geneva are highly fractured and faulted (Guglielmetti et al., 2020) and could therefore be much more permeable than literature and/or measured values. The well pattern is also altered to include an auxiliary well (shown in Figure 1) that produces water during the loading stage, thereby balancing the reservoir pressure. Although only one auxiliary well is simulated, the symmetry of the problem means that this is equivalent to simulating a five-spot well pattern, where the main well sits in the middle of four auxiliary wells. The flow rate into the main well (which is actually one quarter of the total flow rate into the main well due to symmetry) equals the flow rate out of the auxiliary well.

The parameters for the sensitivity analysis are summarized in Table 2, and the surface uplift as a function of distance from the well is shown in Figure 3. For all scenarios, the uplift is largest at the well and decreases as the distance from the well increases. As the distance from the well increases, the uplift decreases at an increasing rate initially, and then hits an inflection point and starts to decrease at a decreasing rate. For the base case scenario, the surface uplift is 6.4 cm at the well, and decreases to <2 cm at 1 km from the well. Injection into the shallow aquifer results in a larger uplift of 11.4 cm directly above the well, which also decreases to <2 cm 1 km from the well and is smaller than the base case at a distance greater than 1 km. For a pliable rock, the uplift is 12.0 cm at the well and remains larger than the base-case uplift at nearly all distances from the well. The uplift is significantly smaller for the permeable aquifer and auxiliary well scenarios, with maximum uplift of ~0.3 cm and <0.1 cm, respectively.

Table 2 – Parameters for sensitivity analysis

Simulation	Target Formation and depth (m)	Young's Modulus (GPa)	$k_{aquifer2}$ (m^2)	Well Pattern
1: Base case	Jurassic, 750	50	10^{-15}	One Well
2: Shallow aquifer	Cretaceous, 500	50	10^{-15}	One Well
3: Pliable rock	Jurassic, 750	10	10^{-15}	One Well
4: Permeable aquifer	Jurassic, 750	50	10^{-13}	One Well
5: Auxiliary well	Jurassic, 750	50	10^{-15}	Five Spot Auxiliary Well Pattern

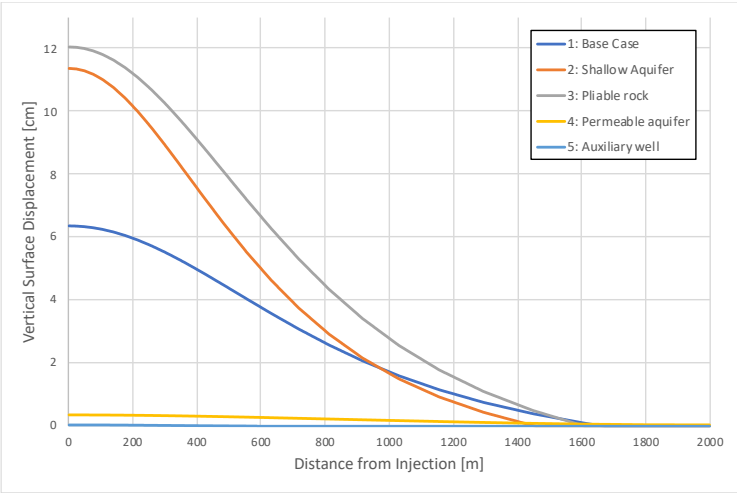

Figure 3: The surface uplift versus the distance from the injection plotted along the line A-A' shown in Figure 2b for the sensitivity analysis scenarios described in Table 2.

5. DISCUSSION AND CONCLUSIONS

Our simulations show that the aquifer permeability (or more accurately, the transmissivity) must be large to avoid excessive pore pressure and uplift. Large aquifer transmissivity has been identified as a key component of successful ATES systems in the past (Snijders and Drijver, 2016). For two reasons, it is likely that the aquifers in Geneva are more permeable than the base-case scenario simulation. Firstly, the fractures and faults in the basin are likely to enhance the permeability. Secondly, the observed artesian flow rate (50 L/s) at GEo-01 is achieved with a modest hydraulic head gradient from the recharge in the nearby Jura mountains, which implies that the permeability near GEo-01 is much larger than 10^{-15} m^2. Nevertheless, there are questions remaining. For example, how does heat storage and ground deformation differ when permeability exists in fractured rock, as seen in Geneva, rather than in a rock matrix, as is typical for ATES? Is permeability large in other parts of the Geneva basin, at locations far from the "flower-structure" faults that GEo-01 is drilled into?

Our results also show that auxiliary well(s) are important to balance the pressure and limit surface deformation. This result makes sense, because the majority of ATES systems use multiple wells (Fleuchaus et al., 2018). This result, in turn, raises questions about how the heat, that is stored between the auxiliary wells, will affect ground surface uplift. For example, what is the optimal spacing between the main and auxiliary wells? Smaller well spacing would require a smaller pressure difference between the wells for any given flow rate. This would give the benefits of less poroelastic uplift and lower pumping costs. But a smaller well spacing would also require the temperature of the reservoir to be increased further to store a given amount of heat, which would result in a larger amount of thermal expansion.

The results here are somewhat preliminary in nature. They highlight that storing large amounts of heat requires large transmissivity and auxiliary well(s) to avoid large poroelastic surface deformation. The depth of the injection and the rock's Young's modulus also play a role in the amount of uplift, but they seem to be of secondary importance. We have not yet included thermal coupling, which is expected to also drive surface deformation. Future work will therefore include THM modeling, longer simulations that include multiple years of loading and unloading cycles, and more site-specific details of the surface and subsurface aspects of the planned Geneva heat storage project. This future work is expected to enable us to answer questions about: (a) the importance of thermal versus poroelastic expansion of the rock matrix upon hot water storage concerning the degree and pattern of ground surface deformation at an HT-ATES system, (b) the optimal layout of the wells to maximize heat storage and minimize ground surface uplift, and (c) the evolution of an HT-ATES system throughout its lifetime and the potential for deformation to reach a pseudo

steady state. The THM approach can also be applied to improve the understanding of surface deformation in the context of geothermal energy, geologic carbon sequestration, and other ATES sites worldwide.

6. ACKNOWLEDGEMENTS

HEATSTORE (170153-4401) is one of nine projects under the GEOTHERMICA – ERA NET Cofund aimed at accelerating the uptake of geothermal energy by 1) advancing and integrating different types of underground thermal energy storage (UTES) in the energy system, 2) providing a means to maximise geothermal heat production and optimise the business case of geothermal heat production doublets, 3) addressing technical, economic, environmental, regulatory and policy aspects that are necessary to support efficient and cost-effective deployment of UTES technologies in Europe.

This project has been subsidized through the ERANET cofund GEOTHERMICA (Project n. 731117), from the European Commission, RVO (the Netherlands), DETEC (Switzerland), FZJ-PtJ (Germany), ADEME (France), EUDP (Denmark), Rannis (Iceland), VEA (Belgium), FRCT (Portugal), and MINECO (Spain). More information can be found on www.heatstore.eu.

REFERENCES

Alger B., Andrš D., Carlsen R. W., Gaston D.R., Kong F., Lindsay A. D., Miller J. M., Permann C. J., Peterson J. W., Slaughter A. E., and Stogner R.: MOOSE Web Page. https://mooseframework.org. (2019).

Biot, M. A.: General three-dimensional theory of poroelasticity. *J. Appl. Phys*, **12**, (2941), 155-164.

Bloemendal, M., Olsthoorn, T., & Boons, F.: How to achieve optimal and sustainable use of the subsurface for Aquifer Thermal Energy Storage. *Energy Policy*, **66**, (2014), 104-114.

Cacace, M., & Jacquey, A. B.: Flexible parallel implicit modelling of coupled thermal–hydraulic–mechanical processes in fractured rocks. *Solid Earth*, **8**(5), (2017), 921-941.

Fialko, Y., & Simons, M.: Deformation and seismicity in the Coso geothermal area, Inyo County, California: Observations and modeling using satellite radar interferometry. *Journal of Geophysical Research: Solid Earth*, **105**(B9), (2000), 21781-21793.

Fleuchaus, P., Godschalk, B., Stober, I., and Blum, P.: Worldwide application of aquifer thermal energy storage–A review. *Renewable and Sustainable Energy Reviews*, **94**, (2018), 861-876.

Hartog, N., Drijver, B., Dinkla, I., & Bonte, M.: Field assessment of the impacts of Aquifer Thermal Energy Storage (ATES) systems on chemical and microbial groundwater composition. *Proceedings*, European Geothermal Conference, Pisa, Italy (2013).

Gaston, D. R., Permann, C. J., Peterson, J. W., Slaughter, A. E., Andrš, D., Wang, Y., ... and Zou, L.: Physics-based multiscale coupling for full core nuclear reactor simulation. *Annals of Nuclear Energy*, **84**, (2015), 45-54.

Guglielmetti, L., Alt-Epping P., Birdsell D., De Oliveira Filho F., Diamond L., Driesner T., Eruteya O., Hollmuller P., Jutzeler M., Makhloufi Y., Martin F., Meier P., Meyer M., Mindel J., Moscariello A., Nawratil De Bono C., Quiquerez L., Sohrabi R., Saar M., Valley B., Van den Heuvel D., and Wanner C.,: HEATSTORE SWITZERLAND: New Opportunities of Geothermal District Heating Network Sustainable Growth by High Temperature Aquifer Thermal Energy Storage Development, *Proceedings*, World Geothermal Congress, Reykjavik, Iceland (2020). Submitted for publication July, 2019.

Poulet, T., & Veveakis, M.: A viscoplastic approach for pore collapse in saturated soft rocks using redback: an open-source parallel simulator for rock mechanics with dissipative feedbacks. Computers and Geotechnics, **74**, (2016), 211-221.

Sarychikhina, O., & Glowacka, E.: Spatio-temporal evolution of aseismic ground deformation in the Mexicali Valley (Baja California, Mexico) from 1993 to 2010, using differential SAR interferometry. *Proceedings of the International Association of Hydrological Sciences*, **372**, (2015), 335-341.

Theis, C. V.: The relation between the lowering of the piezometric surface and the rate and duration of discharge of a well using ground-water storage. *Eos, Transactions American Geophysical Union*, **16**, (2935), 519-524.

Verruijt, A.: Theory and problems of poroelasticity. Delft University of Technology, (2013).

Vogler, D., Walsh, S. D., Rudolf von Rohr, P., & Saar, M. O.: Numerical Simulations of Thermo-Mechanical Processes during Thermal Spallation Drilling for Geothermal Reservoirs. *AGU Fall Meeting Abstracts*, New Orleans, LA (2017).

Wang, H. F.: Theory of linear poroelasticity with applications to geomechanics and hydrogeology. Princeton University Press. (2000).